Investigation of The Improvements in Cavitation And Pressure Pulse Due to The Endplate Propeller

[1] Young-Zehr Kehr; [1] Huan-Jia Xu; [1] Jui-Hsiang Kao*; [1] Yan-Jhang Lin;

[1] *Department of Systems Engineering and Naval Architecture National Taiwan Ocean University Keelung, Taiwan, R.O.C*

Abstract

The aim of this paper is to investigate cavitation and pressure pulse on the stern due to the operating propellers of a container ship. Three optimally designed propellers are tested in this paper. Two propellers are conventional type. The third one is unconventional, and formed by a tip-end plate. These three propellers are design optimally at the same design point, and compared according to the experimental results. The tests are carried out in the large cavitation tunnel of National Taiwan Ocean University (NTOU), and evidence is offered regarding the remarkable improvements in the cavitation extension and the exciting force on the stern achieved by the unconventional propeller.

Keywords: cavitation; pressure pulse; tip-end plate; cavitation tunnel

1. Introduction

Generally, some skills, such as high skew, increasing area ratio, and tip unloading are often applied in conventional propellers to reduce the cavitation. The cavitation of the marine propellers can be classified into several types, and the tip vortex cavitation always appears first. As the tip vortex cavitation is controlled well, the inceptions of other types of cavitation can be delayed.

In Gómez (1976), the ideal of tip loaded propeller was first proposed to restrain the tip vortex cavitation. The tip loaded propeller was shaped by a bent tip, and named as TVF (tip vortex free). Since 1980, Gómez's company, SISTEMAR, has remained devoted to the development of the CLT (Contracted and Loaded Tip) propeller. Gómez and Adalid (1995) derived the New Momentum Theory, which mathematically proves that the induced velocity at the propeller disk of a CLT propeller is much lower than that of a conventional propeller. The ideal efficiency of the CLT propeller is greater than that of the conventional propeller due to the increased contribution of the over-pressure on the pressure side. Some important features of the flow, like the leading edge vortex of skewed blades and the vortex at the outer region of the endplate on the suction side were identified by Antonio et al. (2006). Adalid and Gennaro (2011) proved that CLT propellers grant several significant advantages over conventional propellers, the most important being: (1) 5 to 8% higher efficiency over the entire operation; (2) lower induced noise and vibrations; and (3) Improved ship maneuverability characteristics. Several types of modifications including variations in plate contraction angle, and in plate swept and flap angle are studied in Antonio et al. (2012). Stefano Gaggero and Stefano Brizzolara (2012) conducted numerical computations to predict the development of a smaller sheet cavity bubble (from the leading edge) on the outer side of the tip plate side; the numerical result is qualitatively in agreement with the experimental observations. It is posited by Michael et al. (2014) that the CLT propeller with reduced angle-of-attack loading would have higher efficiency. Stefano et al. (2016) applied tip unloading in the CLT propeller to reduce the tip vortex cavitation; they found that the optimization of the tip plate improves cavity reduction by 10–20%. In this paper, a container ship equipped with three propellers separately is tested in the cavitation tunnel. The improvements in cavitation and pressure pulse on the stern due to the endplate propeller are investigated.

2. Simulated Conditions and Models

Three model propellers (P1, P2, and P3) are tested in this paper. The simulated conditions are as shown in Table 1.

*Corresponding Author, Jui-Hsiang Kao: JHKAO@mail.ntou.edu.tw

Main Engine	M/E Type : MAN B&W 10K98MC DMCR : 41,200 KW x 84.2 RPM
Service Speed	NOR with 15% SM on design draft (Based on BF0, Transmission Efficiency 0.99)
Shaft Immersion (m)	7.6
Ship Speed (kn)	23.35 (P1 propeller)/ 23.38 (P1 propeller)/ 23.39 (P3 propeller)
Shaft Speed (RPS)	1.43 (P1 propeller)/ 1.43 (P1 propeller)/ 1.45 (P3 propeller)
Max. Propeller Diameter (m)	8.7

Table 1. Simulated conditions for the ship

The tested model propellers are list in Table2, and the outlines of these three model propellers are shown in Figure 1. P1 and P2 are conventional type. The area ratio of P2 is increased for reducing the cavitation and exciting force on the stern. P3 is the unconventional type, and with an endplate in order to restrain the tip vortex cavitation.

Model Propeller No	P1	P2	P3
Diameter	269mm	269mm	266mm
Hub Diameter	48mm	48mm	48mm
Pitch-Dia.-Ratio at 0.7R	1.086	1.07	1.073
Blade Area Ratio	0.56	0.663	0.53
No. of Blades	5	5	5

Table 2. The main dimensions for the model propellers

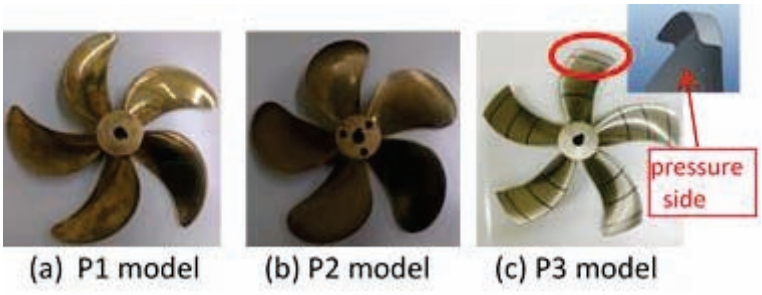

Figure 1. The model propellers

3. Test Arrangements

The tests are carried out in the large cavitation tunnel of NTOU, Figure 2. Its test section is 10m long, 2.6m wide and 1.5m high and allows the installation of the whole ship model. The free surface is substituted by aluminum plates, suppressing the wave system of the model. In order to compensate for the deceleration of the flow due to the boundary layer below these wave suppressing plates, the model draught in the tunnel is increased by 50mm.

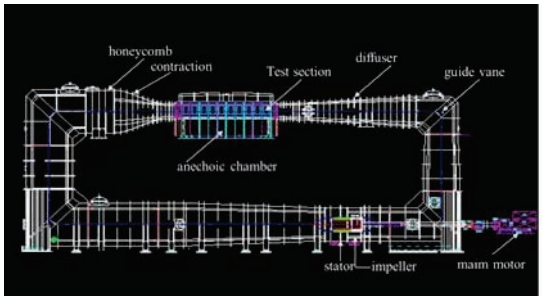

Figure 2 The NTOU large cavitation tunnel

The model scale is 1/32.34. The ship model is equipped with rudder, propeller and shaft line. The stern arrangement is shown in Figure 3.

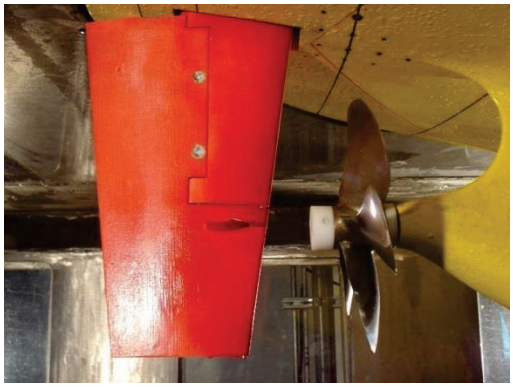

Figure 3 The hull model with model propeller

In the ship model, the R51 dynamometer made by Cusson was equipped to measure the thrust, torque and rotating speed. Eight pressure pick-ups were installed inside the model above the propeller as shown in Figure 4.

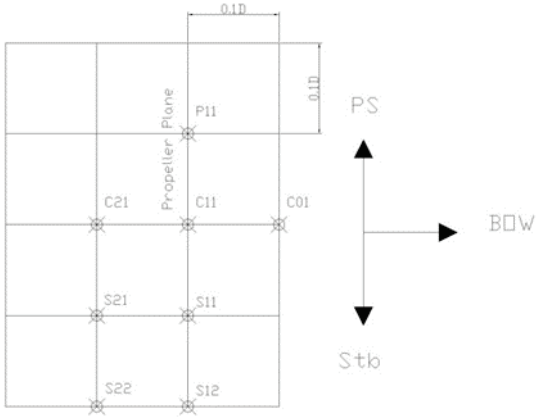

Figure 4 The arranged pressure pick-ups

4. Result of The Propeller Cavitation Observation

The definition for the angular positions of the propeller is given in Figure 5. The cavitation extensions are given in Figures 6 to 8.

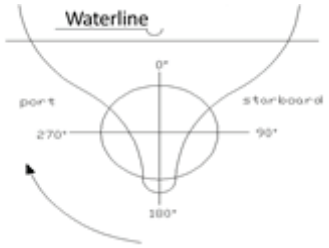

Figure 5 The definition for the angular positions

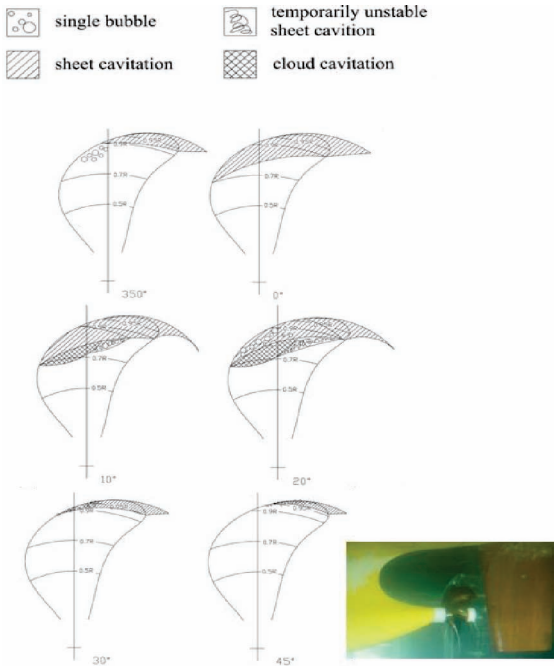

Figure 6 Cavitation phenomena sketches for the P1 propeller

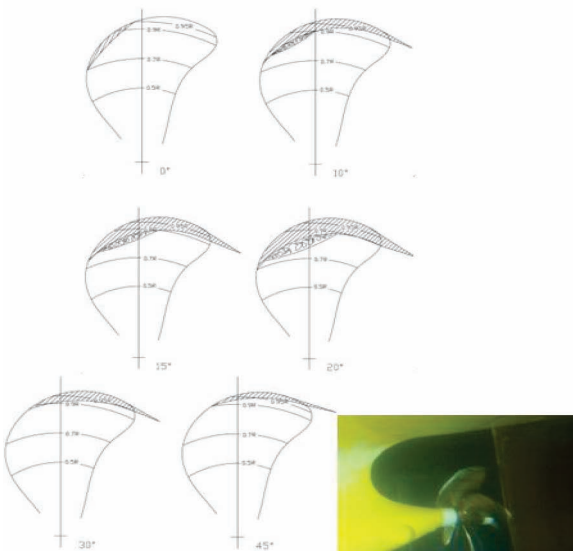

Figure 7 Cavitation phenomena sketches for the P2 propeller

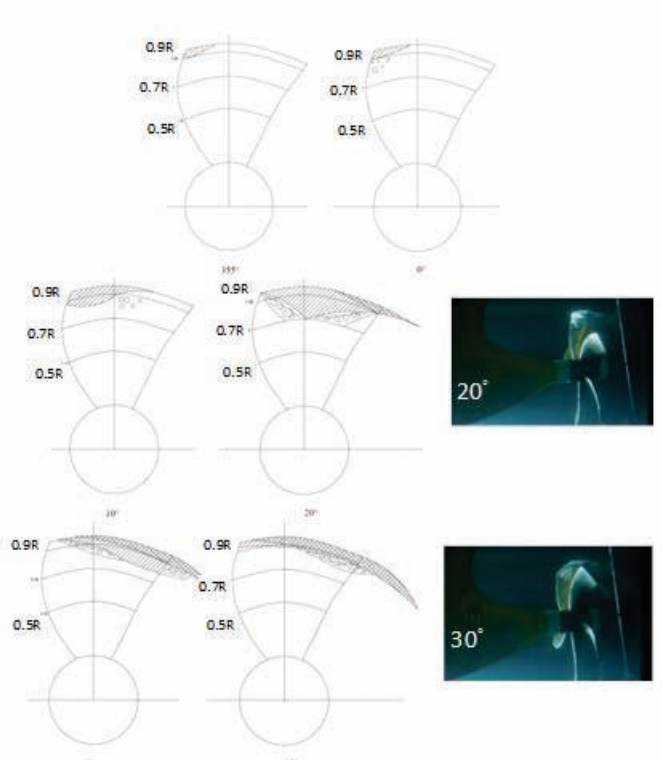

Figure 8 Cavitation phenomena sketches for the P3 propeller

The cavitation extension of P1 appears from 350 to 45 deg. From 0 to 20 deg., sheet cavitation extends from 0.7R, and the thickness of the sheet cavitation is very thick. Because the volume of the sheet cavitation varies very rapidly and complexly; thus, cloud cavitation and unstable sheet cavitation are also found. The cavitation extensions at 10 and 20 deg. nearly cover the whole blade back side from 0.8R. Besides, serious tip vortex cavitation bursting can be found from 10 and 20 deg. The cavitation extension of P2 appears from 0 to 45 deg. As compared with P1, the cavitation extension caused by P2 is smaller and thinner. From 0 to 20 deg., sheet cavitation extends from 0.7R, and some unstable sheet cavitation also appears. Though, the cavitation extensions of P3 are similar with those of P2, the volume of sheet cavitation near the tip of P3 is smaller due to the endplate which effectively reduces the strength of the tip vortex.

5. Result of The Propeller Pulse Measurement

The measured pressure pulses are converted to full-scale ones by using the non-dimensional factor Kp. The conversion is shown in Equation 1.

$$\Delta P_{ship} = \left(K_p\right)_{model} \times \rho {n_{ship}}^2 {D_{ship}}^2 \times \sqrt{2} = \left[\frac{(\Delta P_{model})}{\rho {n_{model}}^2 {D_{model}}^2}\right] \times \rho {n_{ship}}^2 {D_{ship}}^2 \times \sqrt{2} \qquad (1)$$

where ρ is the fluid density, n the shaft speed and D the propeller diameter. In Equation (1) ΔP_{model} is the root-mean-square pressure pulse; thus $\sqrt{2}$ is required to transfer the root-mean-square value to the maximum one, ΔP_{ship}.
The full-scale results are given in Figures 9. Figure 9 shows the P1 propeller causes the highest harmonic amplitude, 9 KPa. The pressure pulse due to P3 propeller is the smallest, 5.5 KPa.

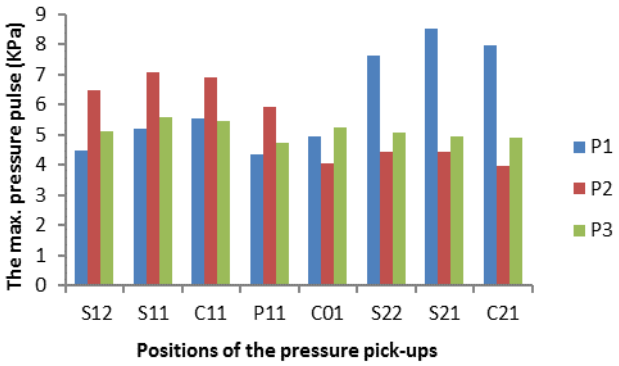

Figure 9 The maximum full-scale amplitude of the pressure pulses for the model propellers

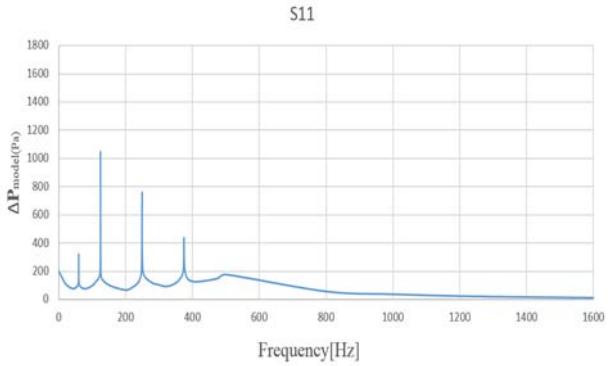

Figure 10 Frequency spectra at pick-up S11 of the P3 model propeller

Figure 10 shows the frequency spectra of P3 model propeller at pick-up S11, having the highest full-scale first harmonic amplitude, 5.5 KPa. It is indicated in Figure 10 that the amplitudes in high frequency decay rapidly, and the blade-rate amplitudes caused by sheet cavitation in low frequency dominate. In other words, the tip vortex cavitation is controlled well; thus, the high-frequency amplitudes disappear.

6. Conclusion and Recommendations

From above results, it is known that the maximum pressure pulse and extended sheet cavitation volume of P3 propeller are less than those of P1 and P2 propellers. Besides, the pressure pulses of P3 propeller at high frequency disappear. The reason for these is due to the endplate which successfully prevents the tip vortex form growing, and reduces the strength of the tip vortex.
It is recommended that the chord lengths near the blade tip should be increased for the P3 propeller in order to restrain the growing of the cavitation volume more.

References

[1] Gómez, G.P. 1976. *Una Innovación en el Proyecto de Hélices*. Ingeniería Naval.
[2] Gómez, G.P. and Adalid, J.G. 1995. *Tip Loaded Propellers (CLT) Justification of Their Advantages Over Conventional Propellers Using the New Momentum Theory*. Report no.429, pp.5-60, SISTEMAR, S.A.Spain.
[3] Antonio Sánchez-Caja, Sipilä, T. P., and Pylkkänen, J.V. 2006. *Simulation of the Incompressible Viscous Flow Around an Endplate Propeller Using a RANSE Solver*. 26th Symposium on Naval Hydrodynamics Rome, Italy, 17-22.
[4] Adalid, J.G., and Gennaro, G. 2011. *Latest experiences with Contracted and Loaded Tip (CLT) propellers. Sustainable Maritime Transportation and Exploitation of Sea Resources*, 1st ed., Vol. 1, Taylor & Francis Group, London, 47-53.
[5] Antonio Sánchez-Caja, J. González-Adalid, M. Pérez-Sobrino, and I. Saisto, 2012. *Study of End-Plate Shape Variations for Tip Loaded Propellers Using a RANSE Solver*. 29th Symposium on Naval Hydrodynamics Gothenburg, Sweden, 26-31.

[6] Stefano Gaggero, and Stefano Brizzolara. 2012. *Endplate effect propellers: A numerical overview. Sustainable Maritime Transportation and Exploitation of Sea Resources* – Rizzuto & Guedes Soares (eds) Taylor & Francis Group, London, ISBN 978-0-415-62081-9.
[7] Michael Brown, Antonio Sánchez-Caja, Juan G. Adalid., Scott Black, Mariano Pérez Sobrino, Phillip Duerr, Seth Schroeder, Ilkka Saisto, and Saisto, I. 2014. *Improving Propeller Efficiency Through Tip Loading*. 30th Symposium on Naval Hydrodynamics Hobart, Tasmania, Australia, 2-7.
[8] Stefano Gaggeroa, Juan Gonzalez-Adalidb, and Mariano Perez SobrinoI. 2016. *Design of Contracted And Tip Loaded Propellers by Using Boundary Element Methods And Optimization Algorithms*. Applied Ocean Research ,55, 102–129.